Laser and Particle Beams (2009), *27*, 157–169. Printed in the USA.

doi:10.1017/S0263034609000226

Effect of laser beam filamentation on second harmonic spectrum in laser plasma interaction

R.P. SHARMA AND P. SHARMA
Centre for Energy Studies, Indian Institute of Technology, New Delhi, India
(RECEIVED 4 May 2008; ACCEPTED 4 December 2008)

Abstract

This paper presents the laser beam filamentation at ultra relativistic laser powers, when the paraxial restriction on the beam is relaxed during the filamentation process. On account of laser beam intensity gradient and background density gradients in filamentary regions, the electron plasma wave (EPW) at pump wave frequency is generated. This EPW is found to be highly localized because of the laser beam filaments. The interaction of the incident laser beam with the EPW leads to the second harmonic generation. The second harmonic spectrum has also been studied in detail, and its correlation with the filamentation of the laser beam has been established. Starting almost with a monochromatic component of laser beam propagation, the second harmonic spectrum becomes more complicated, and broadened when the laser beam propagates further, and filamentation takes place. For the typical laser beam and plasma parameters: laser beam with wave length of 1064 nm, power flux of $10^{18}\,\mathrm{W/cm^2}$, and plasma with temperature 1 KeV, we found that the conversion efficiency equals about $(E_2/E_0) = 8 \times 10^{-3}$, and the spectrum is quite broad, which depends upon the laser beam propagation distance. The results (specifically, the second harmonic spectral feature) presented here may be used for the diagnostics of laser produced plasmas.

Keywords: Electron plasma wave; Filamentation; Second harmonic generation

1. INTRODUCTION

Guiding of intense laser pulses in plasma channels (Davis *et al.*, 2005; Liu *et al.*, 2006) is beneficial to various applications (Chen *et al.*, 2008; Yu *et al.*, 2007; Neff *et al.*, 2006), including harmonic generation (Hafeez *et al.*, 2008; Ozaki *et al.*, 2007, 2008; Liu *et al.*,1993; Huillier & Balcou, 1993; Gibbon, 1997), X-ray lasers (Solem *et al.*,1989; Amendt *et al.*,1991; Lemoff *et al.*,1995; Kuehl *et al.*, 2007; Neumayer *et al.*, 2005), advanced laser-fusion schemes (Canaud *et al.*, 2004; Deutsch *et al.*,1996; Regan *et al.*, 1999; Hora, 2007; Imasaki & Li, 2008), and plasma-based accelerators (Tajima & Dawson, 1979; Baiwen *et al.*, 2004; Giulietti *et al.*, 2005; Kruer, 1988; Shi, 2007; Karmakar & Pukhov, 2007). The process of harmonic generation (Nuzzo *et al.*, 2000) has a strong influence on the nature of laser propagation through the plasma. It allows the penetration of laser power to the overdense region and provides a valuable diagnostics (Merdji *et al.*, 2000) of various plasma processes. Second harmonic generation, for instance, provides information about the linear mode conversion of the laser into a plasma wave near the critical layer. In most laser interactions with homogeneous plasma, odd harmonics of laser frequency are generated (Mori *et al.*, 1993; Zeng *et al.*, 1996). However, second harmonics have been observed in the presence of density gradients (Esaray *et al.*, 1993; Malka *et al.*, 1997). This is due to the laser-induced quiver motion of the electrons across a density gradient, which gives rise to a perturbation in the electron density at the laser frequency. This density perturbation, coupled with the quiver motion of the electrons, produces a source current at the second harmonic frequency. Second harmonic generation has also been related to filamentation (Stamper *et al.*, 1985; Meyer & Zhu, 1987), so, second harmonic radiation was shown to be emitted in a direction perpendicular to the laser beam from filamentary structures in the underdense target corona.

Harmonic generation occurs in the intense short-pulse relativistic regime (at intensities $3 \times 10^{18}\,\mathrm{W\,cm^{-2}}$) as well as in the long-pulse regime (at intensities 10^{18}–$10^{17}\,\mathrm{Wcm^{-2}}$). In the short-pulse regime, the generation of harmonic radiation *via* nonlinear mechanism is a topic of growing interest, both from theoretical and from applicative

Address correspondence and reprint request to: R.P. Sharma, Centre for Energy Studies, Indian Institute of Technology, Delhi 110 016, India. E-mail: rpsharma@ces.iitd.ernet.in

viewpoints. Malka *et al.* (1997) have observed 0.1% conversion efficiency into the second harmonic in plasma created by optical field ionization. Schifano *et al.* (1994) experimentally investigated the properties of the second harmonic emission and tested the effectiveness of this emission as a diagnostics for plasma inhomogenities induced by filamentation. Esarey *et al.* (1993) studied the relativistic harmonic generation by intense lasers. The effect of diffraction on the harmonic generation in the forward direction was considered. Baton *et al.* (1993) observed the second-harmonic generation in the forward direction in underdense plasma. Brandi *et al.* (2006) studied the spectral red shift in the harmonic emissions during the plasma dynamics in the laser focus. Ganeev *et al.* (2007) reported about high order harmonic generation in plasma plumes. Gupta *et al.* (2007) studied the third harmonic generation at ultra relativistic laser powers. Ozaki *et al.* (2006) studied intense harmonic generation at silver ablation. Most of the above mentioned works on harmonic generation deals with the propagation and transmission of laser beams in the paraxial approximation, because in most cases, the divergence angles of the investigated laser beams are very small, and the beam widths of the investigated laser beams are far greater than the wavelength. Therefore, the paraxial wave equation gives an accurate description for wave beams near the axis as long as the beam width remains larger than the radiation wavelength λ throughout the propagation. However, in some experimental situations, it is necessary to go beyond the paraxial approximation, e.g., when working with solid-state lasers or semiconductor injection lasers, which generate wide-angle beams for which the paraxial approximation is not applicable and some corrections are necessary.

In this paper, by considering nonparaxial propagation of the Gaussian laser beam in the plasma, we examine the effect of the relativistic and ponderomotive nonlinearity on the second-harmonic generation. The laser exerts a radial ponderomotive force on the electrons and causes a redistribution of the plasma density. The plasma channel, thus produced, guides the laser beam. Moreover, these nonlinear effects will break the laser pulse into small filamentary structures. As the nonparaxial method has been used here, therefore due to the contribution of the off-axial rays, these main filaments get further divided. Several nonlinear optical processes can be induced inside these divided filaments that affect the process of harmonic generation. Here, we first studied the filamentation of the laser beam by considering the nonparaxial propagation, and then investigated the generation of EPW at pump wave frequency, and the second harmonic generation, when relativistic and ponderomotive nonlinearities are operative. We also studied the spectrum of the second harmonic of the ultra intense laser pulse. The paper is organized as follows. In Section 2, we derived the expression for the effective dielectric constant of the plasma and studied the solution for laser beam propagation. Numerical results are shown for the laser intensity evolution in axial and transverse directions, when relativistic and ponderomotive nonlinearities are operative. In Section 3, we derived the dynamical equation governing the generation of the plasma wave at pump wave frequency. Section 4 is devoted to the study of second harmonic generation, with the power spectrum of second harmonics on account of localization. In the last section, some conclusive comments are given.

2. LASER BEAM PROPAGATION

The wave equation governing the electric field of the laser beam in plasma can be written as

$$\nabla^2\vec{E}_0 = \frac{1}{c^2}\frac{\partial^2\vec{E}_0}{\partial t^2} + \frac{4\pi}{c^2}\frac{\partial\vec{j}}{\partial t}., \tag{1}$$

here $\vec{j}$ is the high-frequency total current density. In writing Eq. (1), we neglected the term $\nabla(E\cdot\nabla\ln\varepsilon)$ which is justified as $\omega_p^2/\omega_0^2\ 1/\varepsilon\ \ln\varepsilon = 1$. Substituting in Eq. (1) the value of $\vec{j}$ and the variation of the electric field in the form

$$\vec{E}_0 = A(x, y, z)\exp[i(\omega_0 t - k_0 z)], \tag{2}$$

one obtains the following relation

$$-k_0^2 A - 2ik_0\frac{\partial A}{\partial z} + \left(\frac{\partial^2}{\partial r^2} + \frac{1}{r}\frac{\partial}{\partial r}\right)A = -\frac{\omega_0^2}{c^2}\varepsilon A \tag{3}$$

here ε is the intensity dependent effective dielectric constant of the plasma (as given in Eq. (8) below), $k_0 = (\omega_0/c)\varepsilon_0^{1/2}$ is the wave number, and A is a complex function of space. We used (following Akhamanov *et al.*, 1968),

$$A = A_0(r, z)\exp[-ik_0 s_0(r, z)], \tag{4}$$

where A_0 and s_0 are real functions of space, and the dielectric constant of the plasma is given by

$$\varepsilon_0 = 1 - \frac{\omega_{p0}^2}{\omega_0^2},$$

where ω_{p0} is the plasma frequency given by $\omega_{p0}^2 = 4\pi n_0 e^2/m_0\gamma$ (e is the charge of an electron, m_0 its rest mass, and n_0 is the density of the plasma electrons in the absence of the laser beam). The relativistic factor can be written as

$$\gamma = \left[1 + \frac{e^2 E_0 E_0^*}{c^2 m_0^2 \omega_0^2}\right]^{1/2} \tag{5}$$

Eq. (3) is valid when there is no change in the plasma density. Following Brandi *et al.* (1993), the relativistic ponderomotive force can be given by

$$F_p = -m_o c^2\nabla(\gamma - 1). \tag{6}$$

https://doi.org/10.1017/S0263034609000226 Published online by Cambridge University Press

Using the electron continuity equation and the current density equation for the second order correction in the electron density equation (with the help of ponderomotive force), the total density can be expressed as

$$n = n_0 + n_2 = n_0\left[1 + \frac{c^2}{\omega_{p0}^2}\left(\nabla^2\gamma - \frac{(\nabla\gamma)^2}{\gamma}\right)\right]. \tag{7}$$

Therefore, the effective intensity dependent dielectric constant of the plasma at pump frequency ω_0 is

$$\varepsilon = \varepsilon_0 + \phi(E_0 \cdot E_0^*), \tag{8}$$

where

$$\phi(E_0 \cdot E_0^*) = \frac{\omega_{p0}^2}{\omega_0^2}\left(1 - \frac{n}{n_0\gamma}\right). \tag{9}$$

Expending the dielectric constant in Eq. (8) around $r = 0$ by a Taylor expansion, one can write

$$\varepsilon = \varepsilon_f + \gamma(\omega_0)r^2, \tag{10}$$

where

$$\varepsilon_f = \varepsilon_0 + \frac{\omega_{p0}^2}{\omega_0^2} \times \left[-\frac{1}{2}\frac{e^2E_{00}^2}{m_0^2\omega_0^2c^2f_0^2} + \frac{c^2}{\omega_{p0}^2}\frac{e^2E_{00}^2}{\gamma_{r=0}^2 m_0^2\omega_0^2c^2r_0^2f_0^4}(\alpha_{00} - 1)\right],$$

and

$$\gamma(\omega_0) = -\frac{\omega_{p0}^2}{\omega_0^2}\frac{e^2E_{00}^2k_0^2r_0^2}{2\gamma_{r=0}^3 m_0^2\omega_0^2c^2f_0^2} \times \left[(\alpha_{00} - 1) + \frac{c^2}{\omega_{p0}^2r_0^2f_0^2}(4\alpha_{02} + \alpha_{00})\right].$$

Here r_0 is the beam radius, and f_0 is the dimensionless beam width parameter given by Eq. (13) below. Substituting Eq. (4) into Eq. (3) and separating the real and imaginary parts, we get

$$2\frac{\partial S_0}{\partial z} + \left(\frac{\partial S_0}{\partial r}\right)^2 = \frac{\omega_0^2}{c^2k_0^2}\gamma(\omega_0) + \frac{1}{k_0^2A_0}\left(\frac{\partial^2A_0}{\partial r^2} + \frac{1}{r}\frac{\partial A_0}{\partial r}\right), \tag{11a}$$

$$\frac{\partial A_0^2}{\partial z} + A_0^2\left(\frac{\partial^2S_0}{\partial r^2} + \frac{1}{r}\frac{\partial S_0}{\partial r}\right) + \frac{\partial S_0}{\partial r}\frac{\partial A_0^2}{\partial r} = 0, \tag{11b}$$

To solve the coupled Eqs. (11a) and (11b), we assume

$$A_0^2 = \left(1 + \frac{\alpha_{00}r^2}{r_0^2f_0^2} + \frac{\alpha_{02}r^4}{r_0^4f_0^4}\right)\frac{E_{00}^2}{f_0^2}e^{-r^2/r_0^2f_0^2} \tag{12a}$$

and

$$S = \frac{S_{00}}{r_0^2} + \frac{S_{02}r^4}{r_0^4} \text{ with } \quad S_{00} = \frac{r^2}{2f_0}\frac{df_0}{dz}. \tag{12b}$$

Further, substituting Eqs. (12a) and (12b) into Eq. (11a), equating the coefficients of r^2 on both sides of the resulting equation, and introducing the normalization distance $\xi = zc/\omega_o r_o^2$, we get the following equation for the beam width parameter:

$$\frac{d^2f_0}{d\xi^2} = \frac{1}{f_0^3}\left(-3\alpha_{00}^2 + 8\alpha_{02} + 1 - 2\alpha_{00}\right) - \frac{\omega_{p0}^2}{\omega_0^2}\frac{e^2E_{00}^2k_0^2r_0^2}{2\gamma^3m_0^2\omega_0^2c^2f_0^2} \times \left[(\alpha_{00} - 1) + \frac{c^2}{\omega_{p0}^2r_0^2f_0^2}(4\alpha_{02} + \alpha_{00})\right]. \tag{13}$$

Analogously equating the coefficients of r^4 on both sides of the resulting equation, we obtain the following equation

$$\frac{\partial S_{02}}{\partial z} = -\frac{2\alpha_{02}}{k_0^2r_0^2f_0^6} - \frac{3\alpha_{02}\alpha_{00}}{2k_0^2r_0^2f_0^6} - \frac{3\alpha_{00}^2}{4k_0^2r_0^2f_0^6} + \frac{eE_{00}^2r_0^2}{m_0^2\omega_0^2c^2k_0^2\gamma^3f_0^6}\left(\frac{-\alpha_{00} + 2\alpha_{02}}{r_0^4f_0^4}\right) + \frac{eE_{00}^2}{4m_0^2\omega_0^2k_0^2c^2\gamma^2}\left(\frac{16\alpha_{02}}{r_0^2f_0^4} - \frac{8\alpha_{00}}{r_0^2f_0^4}\right). \tag{14}$$

Substituting Eqs. (12a) and (12b) into Eq. (11b) for the imaginary part and finding the coefficients of r^2 on both sides of the resulting equation, we obtain the equation for the coefficient α_{00} as

$$\frac{\partial\alpha_{00}}{\partial z} = -\frac{16S_{02}f_0^2}{r_0^2}, \tag{15a}$$

Analogously, the coefficient of r^4 gives equation for α_{02}

$$\frac{\partial\alpha_{02}}{\partial z} = \frac{8S_{02}f_0^2}{r_0^2} - \frac{24\alpha_{00}S_{02}f_0^2}{r_0^2}. \tag{15b}$$

Eqs. (12a) and (12b) describe the intensity profile of the laser beams in the plasma along the radial direction when relativistic and ponderomotive nonlinearities are operative. The intensity profile of both laser beams depends on the beam width parameters f_0 and the coefficients (α_{00} and α_{02}) of r^2 and r^4 in the non-paraxial region. Eq. 13 determines the focusing/defocusing of the laser beams along the distance of propagation in the plasma. In order to have a numerical evaluation of the relativistic and ponderomotive filamentation, in this case, and to evaluate the effect of the change of the parameters of the plasma and the laser beam in the non-paraxial region, the numerical computation of Eqs (13), (14), (15a), and

https://doi.org/10.1017/S0263034609000226 Published online by Cambridge University Press

(15b) has been performed. The coupled equations have been solved for an initially plain wave front, and the numerical results are presented in Figures 1 and 2.

When a laser beam propagates through the plasma, then the density of the plasma will be varying in the channel due to the occurring ponderomotive force. The ponderomotive force results from the lowering of the channel density, therefore the refractive index of the plasma increases and the laser gets focused in the plasma. In Eq. (13), the first term is responsible for the diffraction, while the second and third terms (non-linear terms) on the right-hand side of the equation are responsible for the converging behavior of the beams during the propagation in the plasma. These three terms describe the filament formation and the laser beam propagation in the plasma. Figures 1 and 2 shows the intensity profile in the non-paraxial region. They clearly exhibit the generated filaments of the laser beam in the presence of ponderomotive and relativistic nonlinearity. The following set of laser beam parameters have been used in the numerical calculation: the vacuum wavelength of the laser beam was $\lambda = 1064$ nm, the initial radius of the laser beam was equal to 30 μm; laser power flux equaled 10^{18} W/cm^2. Further $\omega_p = 0.03\omega_0$ and $v_{th} = 0.1c$ were satisfied. For the initial wave front of the beam, the initial conditions used here were $f_0 = 1$ and $df_0/dz = 0$ at $z_- = 0$ and $S_{00} = S_{02} = 0$ at $z = 0$. We have performed numerical calculation for different laser and plasma parameters; Figure 2 gives the intensity profile of the laser beam for different values of the initial laser beam intensity $\alpha\ E_{00}^2$ at a constant value of ω_p. Figure 2 gives the intensity profile of the laser beam at different values of ω_p at a constant value of αE_{00}^2.

3. PLASMA WAVE GENERATION

On account of the change in the background density due to the ponderomotive force and the relativistic effects, the laser beam gets filamented as discussed above. In these filaments, the laser beam intensity is very intense and the plasma density is also changed due to the ponderomotive force. Following the standard procedure, the equation governing the electron plasma wave generation can be written as

$$\frac{\partial^2 N}{\partial t^2} - v_{th}^2 \nabla^2 N + 2\Gamma_e \frac{\partial N}{\partial t} - \frac{e}{m}\nabla\cdot(NE) = \nabla\left[\frac{N}{2}\nabla(VV^*) - V\frac{\partial N}{\partial t}\right], \tag{16a}$$

where $2\Gamma_e$ is the Landau damping factor, v_{th}^2 is the square of the electron thermal speed, E is the sum of the electric vectors of the electromagnetic wave and the self-consistent field, V is the sum of the drift velocities of the electron in the electromagnetic field and the self-consistent field, and m is the relativistic mass of the electrons. The density component varying at the pump wave frequency (N_1) can be

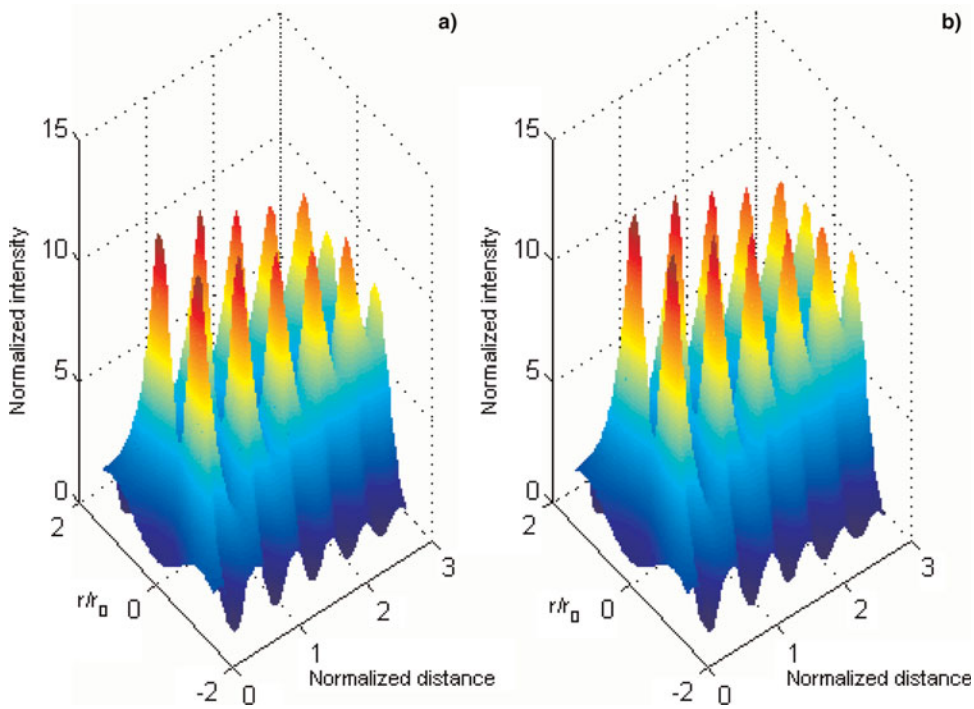

Fig. 1. Variation of laser beam intensity with normalized distance (ξ) and radial distance (r), when relativistic and ponderomotive nonlinearities are operative in the non-paraxial region. Keeping $\omega_p = 0.03\ \omega_0$ constant (**a**) for $\alpha\ E_{00}^2 = 1.0$ (**b**) for $\alpha\ E_{00}^2 = 1.5$.

https://doi.org/10.1017/S0263034609000226 Published online by Cambridge University Press

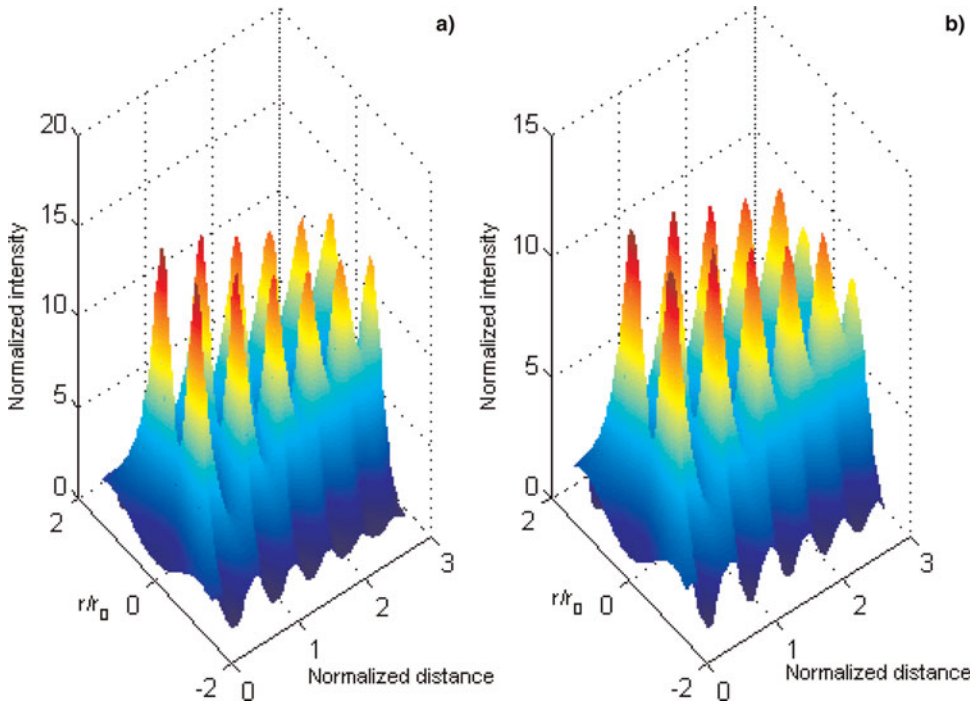

Fig. 2. Variation of laser beam intensity with normalized distance (ξ) and radial distance (r), when relativistic and ponderomotive nonlinearities are operative in the non-paraxial region. Keeping $\alpha\ E_{00}^2 = 1.0$ constant (**a**) for $\omega_p = 0.03\ \omega_0$ (**b**) for $\omega_p = 0.035\ \omega_0$.

written as

$$-\omega_0^2 N_1 + 2i\omega_0\Gamma_e N_1 - v_{th}^2\nabla^2 N_1 + \frac{\omega_{p0}^2}{\gamma}\left(\frac{n}{n_0}\right)N_1 = \frac{e}{m_0\gamma} \times [n\nabla\cdot E_0 + E_0\cdot\nabla n], \tag{16b}$$

where n_0 is the equilibrium electron density, and V_0 is the oscillation velocity of the electron in the pump wave field, and n is the time independent component of the electron density. It is obvious from the source term of Eq. (16b) that the component of N_1 varies when E_0 changes. Therefore N_1 can be written as

$$N_1 = N'_{10}(r, z)e^{-ikz} + N'_{20}(r, z)e^{-ik_0 z} \tag{17}$$

where

$$k^2 = \frac{\omega_0^2 - \omega_{p0}^2}{v_{th}^2},\ k_0 = \frac{\omega_0}{c}\varepsilon_0^{1/2},$$

$N'_{10}(r, z)$ and $N'_{20}(r, z)$ are complex functions of their arguments and satisfy the equations,

$$-\omega_0^2 N'_{10} + 2i\omega_0\Gamma_e N'_{10} + \frac{\omega_{p0}^2}{\gamma}\left(\frac{n}{n_0}\right)N'_{10} - v_{th}^2 \times \left[\left(\frac{\partial^2 N'_{10}}{\partial r^2} + \frac{1}{r}\frac{\partial^2 N'_{10}}{\partial r^2}\right) - 2ik\frac{\partial N'_{10}}{\partial z} - k^2 N'_{10}\right] = 0, \tag{18a}$$

and

$$-\omega_0^2 N'_{20} + 2i\omega_0\Gamma_e N'_{20} + k_0^2 v_{th}^2 + \frac{\omega_{p0}^2}{\gamma}\left(\frac{n}{n_0}\right)N'_{20} = -\frac{N_{0e}e^3E_{00}^3}{4v_{th}^2 m_0^3\gamma\omega_0^2 f_0^3} \times \left(1 + \frac{\alpha_{00}r^2}{r_0^2 f_0^2} + \frac{\alpha_{02}r^4}{r_0^4 f_0^4}\right)^{1/2}\exp\left(-\frac{r^2}{2r_0^2 f_0^2}\right) \times \left[\left(\frac{2\alpha_{00}r}{r_0^2 f_0^2} + \frac{2\alpha_{02}r^3}{r_0^4 f_0^4}\right) - \frac{2r}{r_0^2 f_0^2}\left(1 + \frac{\alpha_{00}r^2}{r_0^2 f_0^2} + \frac{\alpha_{02}r^4}{r_0^4 f_0^4}\right) - \frac{f_0^2 v_{th}^2}{V_{00}^2}\left(\left(1 + \frac{\alpha_{00}r^2}{r_0^2 f_0^2} + \frac{\alpha_{02}r^4}{r_0^4 f_0^4}\right)^{-1}\right) \times \left(\frac{\alpha_{00}r}{r_0^2 f_0^2} + \frac{2\alpha_{02}r^3}{r_0^4 f_0^4}\right) - \frac{r}{r_0^2 f_0^2}\right] \tag{18b}$$

Let the solution of Eqs (18a) and (18b) be written as $N'_{10} = N_{10}(r, z)e^{-iks}$ and $N'_{20} = N_{20}(r, z)e^{-ik_0 s_0}$. Substituting these N'_{10} and N'_{20} in Eqs. (18a) and (18b), respectively, we obtain, after separating the real and imaginary parts

$$\left(\frac{\partial S}{\partial r}\right)^2 + 2\frac{\partial S}{\partial z} = \frac{1}{k^2 N_{10}}\left(\frac{\partial^2 N_{10}}{\partial r^2} + \frac{1}{r}\frac{\partial N_{10}}{\partial r}\right) + \frac{1}{k^2 v_{th}^2}\left(\omega_0^2 - k^2 v_{th}^2 - \frac{\omega_{p0}^2}{\gamma}\left(\frac{n}{n_0}\right)\right), \tag{19a}$$

https://doi.org/10.1017/S0263034609000226 Published online by Cambridge University Press

$$k\frac{\partial N_{10}^2}{\partial z}+N_{10}^2\left(\frac{\partial^2 S}{\partial r^2}+\frac{1}{r}\frac{\partial S}{\partial r}\right)+\frac{\partial S}{\partial r}\frac{\partial N_{10}^2}{\partial r}+\frac{2\Gamma_e\omega_0 N_{10}^2}{v_{th}^2}=0, \quad (19b)$$

and

$$N_{20}\approx-\frac{N_{0e}e^3E_{00}^3\exp(-r^2/2r_0^2f_0^2)}{4v_{th}^2m_0^3\gamma\omega_0^2f_0^3[\omega_0^2-k_0^2v_{th}^2-2i\omega_0\Gamma_e-\omega_{p0}^2n/\gamma n_0]}\times\begin{bmatrix}(2\alpha_{00}r/r_0^2f_0^2+2\alpha_{02}r^3/r_0^4f_0^4)-2r/r_0^2f_0^2\\(1+\alpha_{00}r^2/r_0^2f_0^2+\alpha_{02}r^4/r_0^4f_0^4)\\-f_0^2v_{th}^2/V_{00}^2\\((1+\alpha_{00}r^2/r_0^2f_0^2+\alpha_{02}r^4/r_0^4f_0^4)^{-1})\\(\alpha_{00}r/r_0^2f_0^2+2\alpha_{02}r^3/r_0^4f_0^4)-r/r_0^2f_0^2\end{bmatrix} \quad (20)$$

Following Akhmanov *et al.* (1968), the solution of Eqs (19a) and (19b) can be written as

$$S=\frac{S_{0p}}{a_0^2}+\frac{S_{2p}r^4}{a_0^4},\ \text{with}\quad S_{0p}=\frac{r^2}{2f}\frac{df}{dz}, \quad (21)$$

$$N_{10}^2=\frac{B^2}{f^2}\left(1+\frac{\alpha_{00}r^2}{a_0^2f_0^2}+\frac{\alpha_{02}r^4}{a_0^4f_0^4}\right)\exp\left(-\frac{r^2}{a_0^2f^2}\right)\exp(-k_iz), \quad (22)$$

where $k_i=2\Gamma_e\omega/kv_{th}^2$, and f is the dimensionless width parameter of the plasma wave governed by

$$\frac{d^2f}{d\xi^2}=\left(\frac{r_0}{a_0}\right)^4\left(\frac{k_0}{k}\right)^2\frac{1}{f^3}(-3\alpha_{00}^2+8\alpha_{02}+1+2\alpha_{00})-f\frac{c^2}{v_{th}^2}\left(\frac{k_0}{k}\right)^2\frac{\omega_{p0}^2}{\omega_0^2}\frac{e^2E_{00}^2k_0^2r_0^2}{2\gamma^3m_0^2\omega_0^2c^2f_0^2}\times\left[(1-\alpha_{00})+\frac{c^2}{\omega_{p0}^2r_0^2f_0^2}(4\alpha_{02}+\alpha_{00})\right]. \quad (23)$$

B and a_0 are constants to be determined by the boundary conditions when the amplitude of the generated plasma wave at $z=0$ is zero. Thus

$$B\approx-\frac{N_{0e}e^3E_{00}^3\exp(-r^2/2r_0^2)}{4v_{th}^2m_0^3\gamma\omega_0^2[\omega_0^2-k_0^2v_{th}^2-2i\omega_0\Gamma_e-\omega_{p0}^2n/\gamma n_0](1+\alpha_{0p}r^2/a_0^2+\alpha_{2p}r^4/a_0^4)^{1/2}\exp(-r^2/2a_0^2)}\times\begin{bmatrix}(2\alpha_{00}r/r_0^2+2\alpha_{02}r^3/r_0^4)-2r/r_0^2\\(1+\alpha_{00}r^2/r_0^2f_0^2+\alpha_{02}r^4/r_0^4f_0^4)\\-v_{th}^2/V_{00}^2((1+\alpha_{00}r^2/r_0^2f_0^2+\alpha_{02}r^4/r_0^4f_0^4)^{-1})\\(\alpha_{00}r/r_0^2+2\alpha_{02}r^3/r_0^4)-r/r_0^2\end{bmatrix}$$

and

$$a_0=r_0. \quad (24)$$

In a similar way using Eqs (21) and (22) in Eq. (19a) and equating the coefficients of r^4 on both sides of the equation, we obtain the following equation

$$\frac{\partial S_{2p}}{\partial z}=\frac{(-10\alpha_{0p}\alpha_{2p}+2\alpha_{0p}^3+2\alpha_{0p}^2-4\alpha_{2p})}{2k^2a_0^2f^6}+\frac{\omega_{p0}^2}{\omega_0^2}\frac{e^2E_{00}^2r_0^2}{2\gamma^3m_0^2\omega_0^2c^2k^2f_0^2}\left(\frac{2\alpha_{02}}{r_0^4f_0^4}-\frac{\alpha_{00}}{r_0^4f_0^4}\right)+\frac{eE_{00}^2}{m_0^2\omega_0^2c^2k^2\gamma^2}\left(\frac{4\alpha_{02}}{r_0^2f_0^4}-\frac{2\alpha_{00}}{r_0^2f_0^4}\right). \quad (25)$$

By substituting Eqs (21) and (22) into Eq. (19b) and equating the coefficients of r^2 on both sides of the equation, we obtain the equation for the coefficient α_{0p} as

$$\frac{\partial\alpha_{0p}}{\partial z}=-\frac{16S_{2p}f^2}{a_0^2}, \quad (26)$$

In a similar way, the coefficient of r^4 gives the α_{2p} equation

$$\frac{\partial\alpha_{2p}}{\partial z}=\frac{8S_{2p}f^2}{a_0^2}-\frac{24\alpha_{0p}S_{2p}f^2}{a_0^2}. \quad (27)$$

The initial conditions for f are $f=1$ and $df/dz=0$ (plane wave front) at $z=0$, and $S_{0p}=S_{2p}=0$ at $z=0$. Using Poisson's Equation $\nabla E_1=4\pi eN_1$ one can obtain the electric field vector (E_1) of the plasma wave generated at the frequency ω_0

$$E_1=-\frac{4\pi ei}{k}[G_1\exp(-k_iz/2)\exp(-ikz-is_0)-G_2\exp(-ik_0z-is_0)]\exp(-r^2/2r_0^2f_0^2), \quad (28)$$

where

$$G_1=-\frac{N_{0e}e^3E_{00}^3}{4v_{th}^2m_0^3\gamma\omega_0^2[\omega_0^2-k_0^2v_{th}^2-\omega_{p0}^2n/\gamma n_0](1+\alpha_{0p}r^2/a_0^2+\alpha_{2p}r^4/a_0^4)^{1/2}\exp(-r^2/2a_0^2)}\times\begin{bmatrix}(2\alpha_{00}r/r_0^2+2\alpha_{02}r^3/r_0^4)-2r/r_0^2\\(1+\alpha_{00}r^2/r_0^2f_0^2+\alpha_{02}r^4/r_0^4f_0^4)\\-v_{th}^2/V_{00}^2(1+\alpha_{00}r^2/r_0^2f_0^2+\alpha_{02}r^4/r_0^4f_0^4)^{-1}\\(\alpha_{00}r/r_0^2+2\alpha_{02}r^3/r_0^4)-r/r_0^2\end{bmatrix},$$

and

$$G_2=-\frac{N_{0e}e^3E_{00}^3}{4v_{th}^2m_0^3\gamma\omega_0^2f_0^3[\omega_0^2-k_0^2v_{th}^2-\omega_{p0}^2n/\gamma n_0]}\times\begin{bmatrix}(2\alpha_{00}r/r_0^2f_0^2+2\alpha_{02}r^3/r_0^4f_0^4)-2r/r_0^2f_0^2\\(1+\alpha_{00}r^2/r_0^2f_0^2+\alpha_{02}r^4/r_0^4f_0^4)\\-f_0^2v_{th}^2/V_{00}^2(1+\alpha_{00}r^2/r_0^2f_0^2+\alpha_{02}r^4/r_0^4f_0^4)^{-1}\\(\alpha_{00}r/r_0^2f_0^2+2\alpha_{02}r^3/r_0^4f_0^4)-r/r_0^2f_0^2\end{bmatrix}.$$

Eq. (28) gives the expression for the electric field of the excited plasma wave at pump wave frequency (ω_0) in the non-paraxial region. We solved Eq. (28) numerically along with the numerical computation of Eqs (23), (24), (25), (26), (27) to

https://doi.org/10.1017/S0263034609000226 Published online by Cambridge University Press

obtain the variation in electric field at finite z. For the calculations, the same set of parameters has been used as was chosen in Section 2, to study the effect of both nonlinearities on the EPW in the non-paraxial region. The results are presented in Figures 3 and 4. Eq. (28) clearly shows that the electric field of the EPW not only depends on the parameters of the laser beams and their beam width parameters, but also on the coefficients of r^2 and r^4 (α_{00}, α_{02}) and (α_{0p}, α_{2p}). Figure 3 displays the variation of the electric field of the EPW with the distance of propagation and the radial distance in the non-paraxial region with different value of αE_{00}^2 at a constant value of ω_p and Figure 4 gives the EPW profile for different value of ω_p at a constant value of αE_{00}^2. It depicts that the EPW has also a spitted profile with minimum power on the axis.

The dependence of $E(\omega_0)$ on the coefficient of r^2 and r^4 gives the spitted profile of the power of the excited EPW in the non-paraxial region. Figures 3 and 4 shows the variation of the electric field of the plasma wave $|E|^2/|E_{00}|^2$ with the distance of propagation and the radial distance. It is evident from the figures that the EPW gets excited due to nonlinear coupling with the high power laser beam because of the ponderomotive and relativistic nonlinearity. This coupling is so strong that the initial plasma wave becomes highly localized as shown in Figures 3 and 4; it is obvious from Eq. (16b) that the plasma wave amplitude at pump wave frequency depends upon (1) the transverse gradient of the pump wave intensity and (2) the transverse density gradient. For an initially Gaussian laser beam, the transverse intensity gradient is negative while, on account of redistribution of electrons by the ponderomotive force, the density gradient is positive. When the scale of the transverse density gradient is equal in magnitude to the scale of the intensity gradient, the source term of Eq. (16b) becomes zero and one does not expect any plasma wave generation, as it is clear by Eq. (22) with the expression of B. When $z > 0$ is satisfied, the intensity of the laser beam is changing due to filamentation and hence, the density gradient also changes when the laser beam propagates.

4. SECOND HARMONIC GENERATION

Using Eq. (1), one can obtain the second harmonic field by the laser beam. Eq. (1) may be spitted into formulae for the vector potentials of the fundamental mode (A_0) and the second harmonic (A_2),

$$\nabla^2 A_0 + \frac{\omega_0^2}{c^2}\varepsilon_F(\omega_0)A_0 = 0, \tag{29}$$

and

$$\nabla^2 A_2 + \frac{\omega_2^2}{c^2}\varepsilon_2(\omega_2)A_2 = \frac{\omega_{p0}^2}{c^2}\frac{N_1}{n_0}A_0, \tag{30}$$

where $\omega_2 = 2\omega_0$, $\varepsilon_F(\omega_0)$ and $\varepsilon_2(\omega_2)$ are the effective dielectric constants of the plasma at the fundamental and second harmonic frequency, respectively. The dielectric constant at the fundamental mode reads

$$\varepsilon_F(\omega_0) = \varepsilon_f(\omega_0) + \gamma(\omega_0)r^2, \tag{31}$$

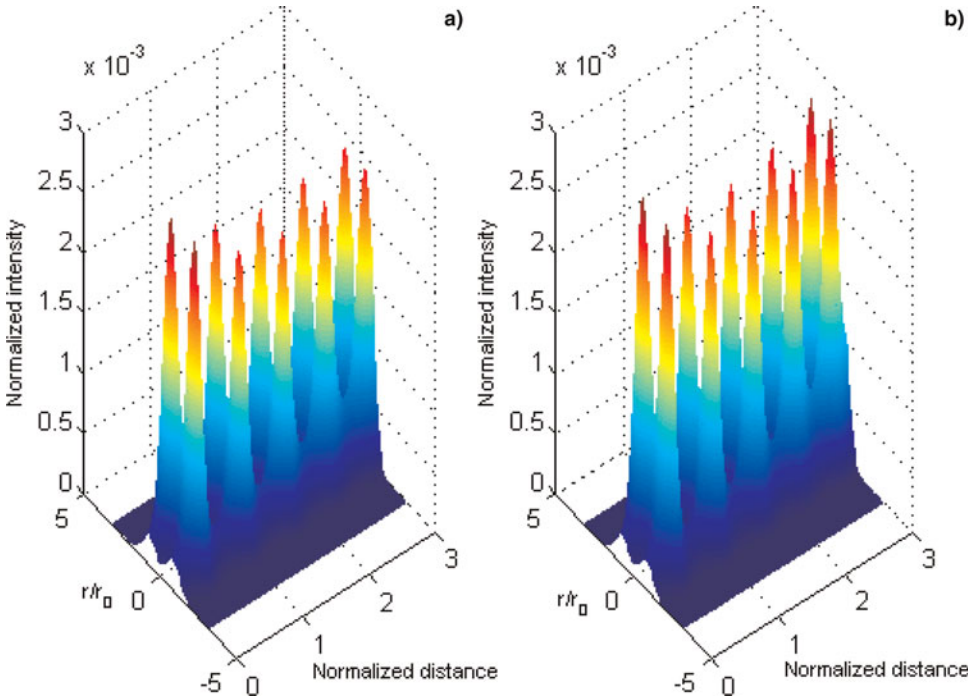

Fig. 3. Variation of the electric field of the electron plasma wave $|E|^2/|E_{00}|^2$ with normalized distance (ξ) and radial distance (r), when relativistic and ponderomotive nonlinearities are operative in the non-paraxial region. Keeping $\omega_p = 0.03\ \omega_0$ constant (**a**) for $\alpha\ E_{00}^2 = 1.0$ (**b**) for $\alpha\ E_{00}^2 = 1.5$.

https://doi.org/10.1017/S0263034609000226 Published online by Cambridge University Press

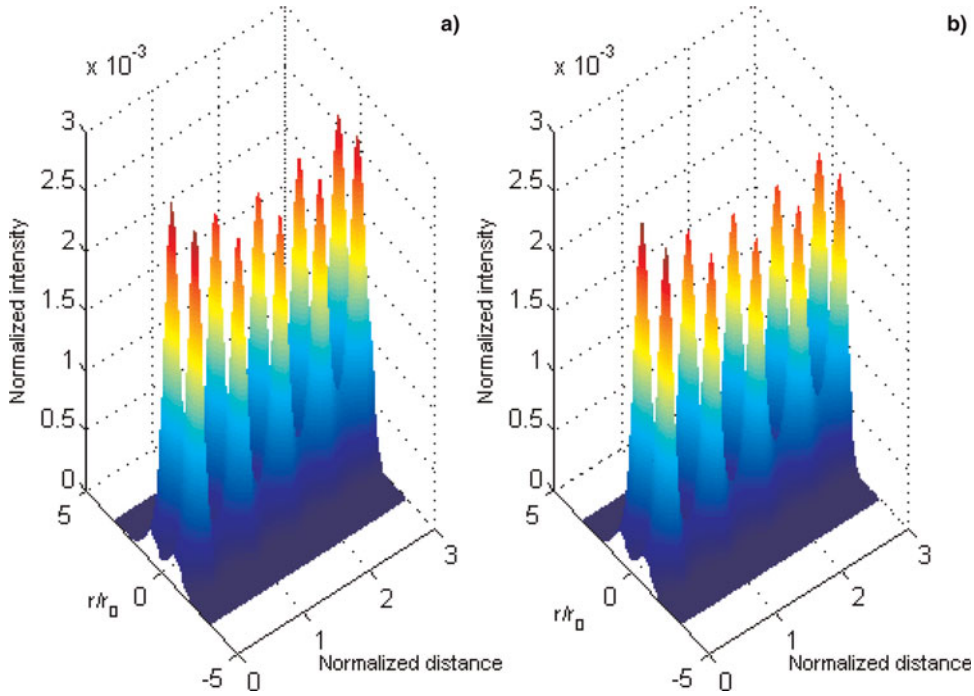

Fig. 4. Variation of the electric field of the electron plasma wave $|E|^2/|E_{00}|^2$ with normalized distance (ξ) and radial distance (r), when relativistic and ponderomotive nonlinearities are operative in the non-paraxial region. Keeping $\alpha\, E_{00}^2 = 1.0$ constant (**a**) for $\omega_p = 0.03\ \omega_0$ (**b**) for $\omega_p = 0.035\ \omega_0$.

where

$$\varepsilon_f = \varepsilon_0 + \frac{\omega_{p0}^2}{\omega_0^2} \times \left[-\frac{1}{2}\frac{e^2E_{00}^2}{m_0^2\omega_0^2c^2f_0^2} + \frac{c^2}{\omega_{p0}^2}\frac{e^2E_{00}^2}{\gamma_{r=0}^2 m_0^2\omega_0^2c^2r_0^2f_0^4}(1-\alpha_{00}) \right],$$

and

$$\gamma(\omega_0) = -\frac{\omega_{p0}^2}{\omega_0^2}\frac{e^2E_{00}^2\,k_0^2r_0^2}{2\gamma^3 m_0^2\omega_0^2c^2f_0^2} \times \left[(1-\alpha_{00}) + \frac{c^2}{\omega_{p0}^2r_0^2f_0^2}(4\alpha_{02}+\alpha_{00}) \right],$$

The dielectric constant at the generation of the second harmonic is

$$\varepsilon_2(\omega_2) = \varepsilon_{2f}(\omega_2) + \gamma(\omega_2)r^2. \tag{32}$$

Here

$$\varepsilon_f(\omega_2) = \varepsilon_0 + \frac{\omega_{p0}^2}{\omega_2^2}\left[-\frac{1}{2}\frac{e^2E_{00}^2}{m_0^2\omega_0^2c^2f_0^2} + \frac{c^2}{\omega_{p0}^2}\frac{e^2E_{00}^2}{\gamma_{r=0}^2 m_0^2\omega_0^2c^2r_0^2f_0^4}(1-\alpha_{00}) \right]$$

and

$$\gamma(\omega_2) = -\frac{\omega_{p0}^2}{\omega_2^2}\frac{e^2E_{00}^2k_0^2r_0^2}{2\gamma^3 m_0^2\omega_0^2c^2f_0^2} \times \left[(1-\alpha_{00}) + \frac{c^2}{\omega_{p0}^2r_0^2f_0^2}(4\alpha_{02}+\alpha_{00}) \right].$$

The solution for the fundamental Eq. (29) can be written as $A_0 = A_0^{'} \exp(-i(k_0z + S_0))$,

$$A_0'^2 = \left(1 + \frac{\alpha_{00}r^2}{r_0^2f_0^2} + \frac{\alpha_{02}r^4}{r_0^4f_0^4}\right)\frac{E_{00}^2}{f_0^2}e^{-r^2/r_0^2f_0^2} S = \frac{S_{00}}{r_0^2} + \frac{S_{02}r^4}{r_0^4} \quad \text{with} \quad S_{00} = \frac{r^2}{2f_0}\frac{df_0}{dz}.$$

where f_0 is described by Eq (13) with the initial condition given in Section 2. The solution of Eq. (30) can be written as

$$A_2 = A_{20}'(r,z)e^{-ik_2z} + A_{21}'(r,z)e^{-2ik_0z}. \tag{33}$$

Using this, we obtain after separating the real and

https://doi.org/10.1017/S0263034609000226 Published online by Cambridge University Press

imaginary parts

$$\frac{\partial^2 A_{21}}{\partial z^2} - 4k_0^2 A_{21} - 8k_0 A_{21}\frac{\partial S_0}{\partial z} + \frac{\partial^2 A_{21}}{\partial r^2} - 4A_{21}\left(\frac{\partial S_0}{\partial z}\right)^2 - 4A_{21}\left(\frac{\partial s_0}{\partial r}\right)^2 + \frac{1}{r}\frac{\partial A_{21}}{\partial r} + \frac{\omega_2^2}{c^2}\left(1 - \frac{\omega_{p0}^2}{\omega_2^2}\right)A_{21} = \frac{\omega_2^2}{c^2}\frac{N_1}{n_0}A_0 \tag{34a}$$

and

$$-4k_0\frac{\partial A_{21}}{\partial z} - 4\frac{\partial A_{21}}{\partial z}\frac{\partial S_0}{\partial z} - 2A_{21}\frac{\partial^2 S_0}{\partial z^2} - 4\frac{\partial A_{21}}{\partial r}\frac{\partial S_0}{\partial r} - 2A_{21}\frac{\partial^2 S_0}{\partial r^2} - 2A_{21}\frac{\partial S_0}{\partial r} = 0, \tag{34b}$$

It must be mentioned here that in writing Eq. (34b) we have taken only that component of N_1 which arises on account of the source term of Eq. (16b) because it is not Landau damped. Furthermore we write

$$A'_{20} = A_{20}(r, z)e^{-ik_2 S_2} \quad \text{and} \quad A'_{21} = A_{21}(r, z)e^{-2ik_0 S_0}. \tag{35}$$

To analyze Eq. (34a), we use Eq. (35), and we get

$$2k_2\left(\frac{\partial S_2}{\partial z}\right) + \left(\frac{\partial S_2}{\partial r}\right)^2 = \frac{1}{A_{20}}\left[\frac{1}{r}\frac{\partial A_{20}}{\partial r} + \frac{\partial^2 A_{20}}{\partial r^2}\right] + \frac{\omega_2^2}{c^2}\left(1 - \frac{\omega_{p0}^2}{\omega_2^2}\right) - \frac{\omega_2^2}{c^2}\frac{N'_{20}}{n_0}\frac{A_{00}}{A_{20}}, \tag{36a}$$

$$k_2\frac{\partial A_{20}^2}{\partial z} + A_{20}^2\left(\frac{\partial^2 S_2}{\partial r^2} + \frac{1}{r}\frac{\partial S_2}{\partial r}\right) + \frac{\partial S_2}{\partial r}\frac{\partial A_{20}^2}{\partial r} = 0. \tag{36b}$$

Considering Eq. (34b), using $A'_{21} = A_{21}e^{-2ik_0 S_0}$, we find

$$A_{21} \cong \frac{\omega_{p0}^2}{c^2}\frac{\omega_2}{\omega_0}\left(\frac{N'_{20}}{n_0}\right)\frac{E_{00}}{f_0}\left(1 + \frac{\alpha_{0h}r^2}{b_0^2 f_2^2} + \frac{\alpha_{2h}r^4}{b_0^4 f_2^4}\right) \times \frac{\exp(-r^2/b_0^2 f_2^2)}{[k_2^2 - 4k_0^2]}. \tag{36c}$$

Let the solution of Eqs (36a) and (36b) be

$$S_2 = \frac{S_{0h}}{b_0^2} + \frac{S_{2h}r^4}{b_0^4} \quad \text{with} \quad S_{0h} = \frac{r^2}{2f_2}\frac{df_2}{dz}.$$
$$A_{20}^2 = \frac{(B')}{f_2^2}\left(1 + \frac{\alpha_{0h}r^2}{b_0^2 f_2^2} + \frac{\alpha_{2h}r^4}{b_0^4 f_2^4}\right)\exp\left(-\frac{r^2}{b_0^2 f_2^2}\right). \tag{37}$$

Here b_0 is the second harmonic beam width. Further we use the initial conditions $df_2/dz = 0$, $f_2 = 1$ at $z = 0$, and $S_{0h} = S_{2h} = 0$ at $z = 0$. f_2 is the dimensionless

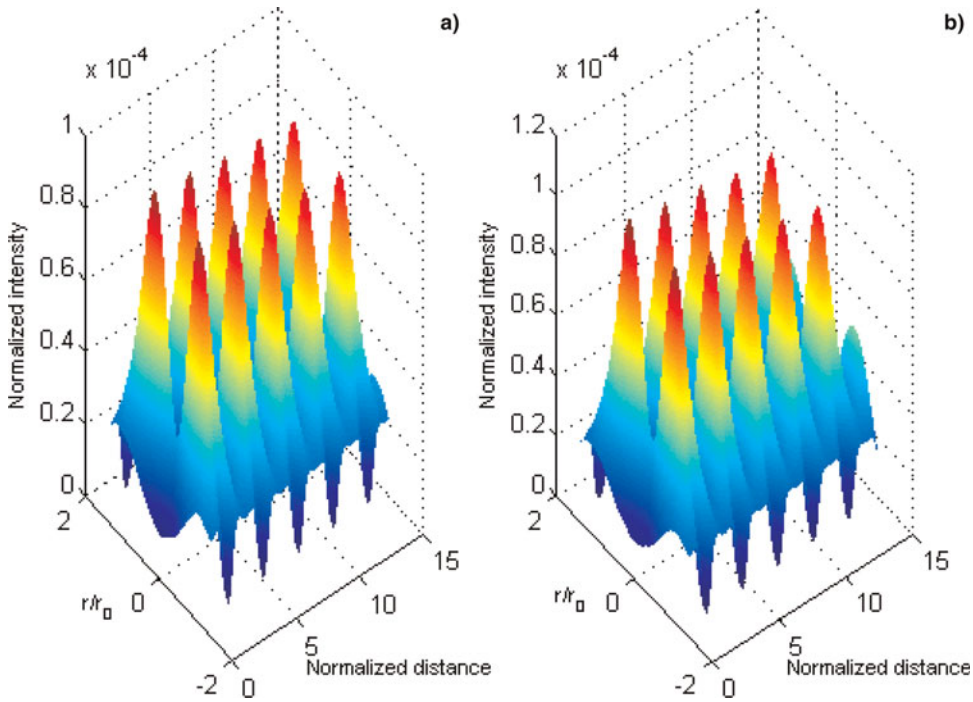

Fig. 5. Variation of the electric field of the generated second harmonic $|E_2|^2/|E_{00}|^2$ with normalized distance (ξ) and radial distance (r), when relativistic and ponderomotive nonlinearities are operative in the non-paraxial region. Keeping $\omega_p = 0.03\ \omega_0$ constant (**a**) for $\alpha\ E_{00}^2 = 1.0$ (**b**) for $\alpha\ E_{00}^2 = 1.5$.

https://doi.org/10.1017/S0263034609000226 Published online by Cambridge University Press

width parameter of the second harmonic radiation, given by

$$\frac{d^2 f_2}{d\xi^2} = \left(\frac{r_0^4}{b_0^4}\right)\left(\frac{k_0^2}{k_2^2}\right)\frac{1}{f_2^3}(-3\alpha_{0h}^2 + 8\alpha_{2h} + 1 + 2\alpha_{0h}) - f_2\frac{c^2}{v_{th}^2}\left(\frac{k_0}{k_2}\right)^2\frac{\omega_{p0}^2}{\omega_2^2}\frac{e^2E_{00}^2k_0^2r_0^2}{2\gamma^3m_0^2\omega_0^2c^2f_0^2} \times\left[(1-\alpha_{00}) + \frac{c^2}{\omega_{p0}^2r_0^2f_0^2}(4\alpha_{02}+\alpha_{00})\right]. \quad (38)$$

Similarly, using Eq. (37) in Eq. (36a) and equating the coefficients of r^4 on both sides of the equation, we obtain the following equation

$$\frac{\partial S_{2h}}{\partial z} = \frac{(-10\alpha_{0h}\alpha_{2h} + 2\alpha_{0h}^3 + 2\alpha_{0h}^2 - 4\alpha_{2h})}{2k_2^2b_0^2f_2^6} + \frac{\omega_{p0}^2}{\omega_2^2}\frac{e^2E_{00}^2r_0^2}{2\gamma^3m_0^2\omega_0^2k_2^2c^2f_0^2}\left(\frac{2\alpha_{02}}{r_0^4f_0^4} - \frac{\alpha_{00}}{r_0^4f_0^4}\right) + \frac{eE_{00}^2}{m_0^2\omega_2^2c^2k_2^2\gamma^2}\left(\frac{4\alpha_{02}}{r_0^2f_0^4} - \frac{2\alpha_{00}}{r_0^2f_0^4}\right). \quad (38a)$$

By substituting Eq. (37) into Eq. (36b) and equating the coefficients of r^2 on both sides of equation, we obtain the equation for the coefficient α_{0h} as

$$\frac{\partial\alpha_{0h}}{\partial z} = -\frac{16S_{2h}f_2^2}{b_0^2}, \quad (38b)$$

In a similar way, the coefficient of r^4 gives the equation for α_{2h}.

$$\frac{\partial\alpha_{2h}}{\partial z} = \frac{8S_{2p}f_2^2}{b_0^2} - \frac{24\alpha_{0h}S_{2h}f_2^2}{b_0^2}. \quad (38c)$$

The constants B' and b_0 are also determined by the boundary condition that the second harmonic generation is zero at $z = 0$

$$B' \approx -\frac{N_{0e}e^3E_{00}^3e^{-r^2/2r_0^2}\times\begin{bmatrix}(2\alpha_{00}r/r_0^2 + 2\alpha_{02}r^3/r_0^4) - 2r/r_0^2\\ (1+\alpha_{00}r^2/r_0^2f_0^2 + \alpha_{02}r^4/r_0^4f_0^4)\\ -v_{th}^2/V_{00}^2(1+\alpha_{00}r^2/r_0^2f_0^2 + \alpha_{02}r^4/r_0^4f_0^4)^{-1}\\ (\alpha_{00}r/r_0^2 + 2\alpha_{02}r^3/r_0^4) - r/r_0^2\end{bmatrix}}{4v_{th}^2m_0^3\gamma\omega_0^2\begin{bmatrix}\omega_0^2 - k_0^2v_{th}^2 - 2i\omega_0\Gamma_e\\ -\omega_{p0}^2n/\gamma n_0\end{bmatrix}\times(1+\alpha_{0h}r^2/b_0^2 + \alpha_{2h}r^4/b_0^4)^{1/2}e^{-r^2/2b_0^2}[k_2^2 - 4k_0^2]} \quad (39)$$

and $b_0 = r_0$

Using Eqs (36c), (37), (38), and (39) in Eq. (33), we get

$$A_2 = -E_{00}\left(\frac{\omega_{p0}^2}{c^2}\right)\left[\frac{H_1}{f_2}e^{-(r^2/2b_0^2f_2^2 + r^2/2r_0^2)}e^{-i(S_2+k_2z)} - \frac{H_2}{f_0^3}e^{-(r^2/2b_0^2f_2^2 + r^2/r_0^2f_0^2)}e^{-2i(k_0z+S_0)}\right]. \quad (40)$$

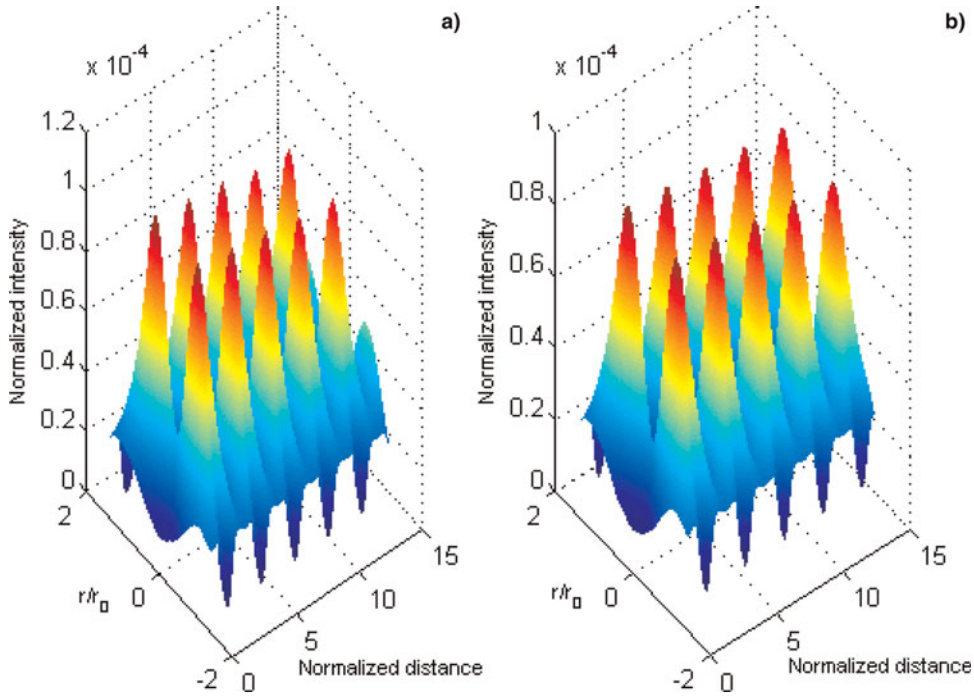

Fig. 6. Variation of the electric field of the generated second harmonic $|E_2|^2/|E_{00}|^2$ with normalized distance (ξ) and radial distance (r), when relativistic and ponderomotive nonlinearities are operative in the non-paraxial region. Keeping $\alpha\, E_{00}^2 = 1.0$ constant (**a**) for $\omega_p = 0.03\ \omega_0$ (**b**) for $\omega_p = 0.035\ \omega_0$.

https://doi.org/10.1017/S0263034609000226 Published online by Cambridge University Press

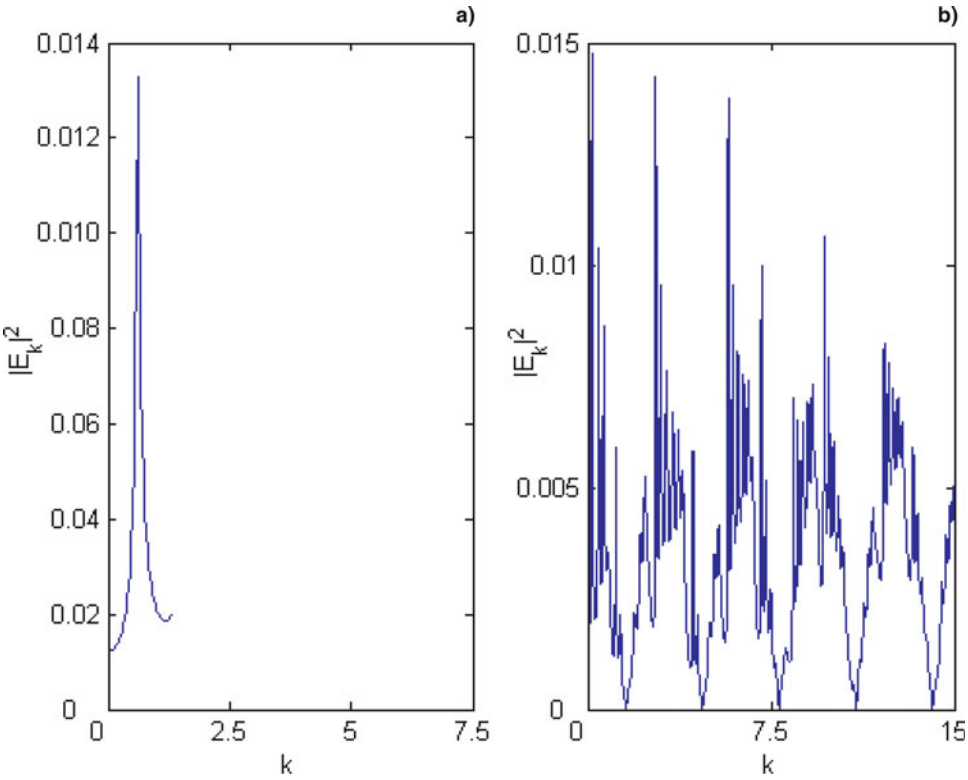

Fig. 7. Power spectrum ($|E_k|^2$ *vs.* k) of the second harmonic generated, when relativistic and ponderomotive nonlinearities are operative in the non-paraxial region. (**a**) In early stages of laser beam propagation, i.e., before filament formation (**b**) after laser beam filament formation.

Here

$$H_1 = -\frac{\begin{array}{l} e^3E_{00}^3(1+\alpha_{00}r^2/r_0^2+\alpha_{02}r^4/r_0^4) \\ \times\left[\begin{array}{l}(2\alpha_{00}r/r_0^2+2\alpha_{02}r^3/r_0^4)-2r/r_0^2 \\ (1+\alpha_{00}r^2/r_0^2f_0^2+\alpha_{02}r^4/r_0^4f_0^4) \\ -v_{th}^2/V_{00}^2(1+\alpha_{00}r^2/r_0^2f_0^2+\alpha_{02}r^4/r_0^4f_0^4)^{-1} \\ (\alpha_{00}r/r_0^2+2\alpha_{02}r^3/r_0^4)-r/r_0^2\end{array}\right] \end{array}}{\begin{array}{l} 4v_{th}^2m_0^3\gamma_{r=0}\omega_0^2[\omega_0^2-k_0^2v_{th}^2-2i\omega_0\Gamma_e-\omega_{p0}^2n/\gamma n_0] \\ \times(1+\alpha_{0h}r^2/b_0^2+\alpha_{2h}r^4/b_0^4)^{1/2} \\ \exp(-r^2/2b_0^2)[k_2^2-4k_0^2]\end{array}}$$

and

$$H_2 = -\frac{\omega_2}{\omega_0}\frac{\begin{array}{l} e^3E_{00}^3(1+\alpha_{00}r^2/r_0^2+\alpha_{02}r^4/r_0^4) \\ \times\left[\begin{array}{l}(2\alpha_{00}r/r_0^2f_0^2+2\alpha_{02}r^3/r_0^4f_0^4)-2r/r_0^2f_0^2 \\ (1+\alpha_{00}r^2/r_0^2f_0^2+\alpha_{02}r^4/r_0^4f_0^4) \\ -f_0^2v_{th}^2/V_{00}^2(1+\alpha_{00}r^2/r_0^2f_0^2+\alpha_{02}r^4/r_0^4f_0^4)^{-1} \\ (\alpha_{00}r/r_0^2f_0^2+2\alpha_{02}r^3/r_0^4f_0^4)-r/r_0^2f_0^2\end{array}\right] \end{array}}{\begin{array}{l} 4v_{th}^2m_0^3\gamma\omega_0^2f_0[\omega_0^2-k_0^2v_{th}^2-2i\omega_0\Gamma_e-\omega_{p0}^2n/\gamma n_0] \\ \times[k_2^2-4k_0^2]\end{array}}.$$

We have developed the theory of second harmonic generation and derived the expression for the electric field of the second harmonic when relativistic and ponderomotive nonlinearities are operative. Figure 5 shows the variation of the electric field of the second harmonic with normalized distance and radial distance for different values of αE_{00}^2 at a constant value of ω_p, and Figure 6 gives the second harmonics' profile with different value of ω_p at a constant value of αE_{00}^2.

We have also studied the spectrum of the second harmonic generated by the ultra intense laser pulse. This $|E_k|^2$ *versus* k plot clearly shows the broadened spectra of the generated harmonic. As it is clear from the power spectrum of the second harmonic, in the initial stages of laser beam propagation a single line is obtained (Fig. 7a). As expected, the main harmonic line is at $k_2 - 2k_0$. For the typical laser parameters, a normalized value of $k_2 - 2k_0$ comes out to be; 1.24. In the wave number spectrum (Fig. 7b) this line is clearly visible. As the wave starts propagating further and filament formation is taking place, the second harmonic spectrum starts becoming broadened, which means new k components are also generated. This is on account of the localization of the second harmonic. As one can see in the initial stages of the laser beam propagation, the generated second harmonic is almost a plane wave but after the filament formation of the laser beam, the spectrum starts broadening.

6. CONCLUSION

In this work, the theory of filamentation of the high power laser beam when relativistic and ponderomotive nonlinearities are operative has been developed by considering the

https://doi.org/10.1017/S0263034609000226 Published online by Cambridge University Press

nonparaxial part of the beam. In the presence of these modified filamentary structures, the plasma wave localization at pump wave frequency has been studied. In case of an ultra intense Gaussian laser beam, the plasma gets depleted from the high field region to the low field region, on account of the relativistic and ponderomotive nonlinearity, and hence a transverse (with respect to the direction of propagation) density gradient is established. When the electric vector of the laser beam is parallel to this density gradient, an EPW at pump wave frequency is generated. In addition to this, the transverse intensity gradient of the laser beam also contributes significantly to the EPW generation. The plasma wave at pump wave frequency has two components; one has the propagation vector $k_0 = \omega_0/c$ and the second has its propagation vector $k \approx \left[\left(\omega_0^2 - \omega_{p0}^2\right)/v_{th}^2\right]^{1/2}$, the phase velocity of the second component depends on ω_{p0}/ω_0; this may be comparable to the thermal speed of the electron and hence this component can undergo Landau damping. But the phase velocity of the first component is the same as that of the pump wave and hence, its Landau damping is negligible. This component contributes significantly to the second harmonic generation on account of its interaction with the pump laser beam. Therefore, it is concluded that at those positions, where the laser beam intensity gradient and the density gradient balance each other, there is no plasma wave generation, but when the intensity gradient dominates over the density gradient then the EPW is generated, as it is shown by the electric field variation of this EPW with normalized distance and radial distance in Figure 3 and 4. Interaction of this plasma wave with the incident laser beam leads to second harmonic generation. We have also studied the spectrum of second harmonics generated by the ultra intense laser pulse. It is seen that in the initial stages of the laser beam propagation, the generated second harmonic is almost a plane wave, but after the filament formation of the laser beam, the spectrum of the second harmonics starts broadening. Therefore, this mechanism may be a good source of second harmonic generation and the spectral features mentioned here may be used for diagnostics of laser produced plasmas.

ACKNOWLEDGMENTS

This work was partially supported by DST, Government of India. One of the authors (Prerana Sharma) is grateful to AICTE for providing the assistance for the present work.

REFERENCES

Akhmanov, S.A., Sukhorukov, A.P. & Khokhlov, R.V. (1968). Self-focusing and diffraction of light in a nonlinear medium. *Soviet Phys. Usp*. **10**, 609–636.

Amendt, P., Eder, D.C. & Wilks, S.C. (1991). X-Ray lasing by optical field induced ionization. *Phys. Rev. Lett*. **66**, 2589–2592.

Baiwen, L.I, Ishiguro, S., Škoric, M.M., Takamaru, H. & Sato, T. (2004). Acceleration of high-quality, well-collimated return beam of relativistic electrons by intense laser pulse in a low-density plasma. *Laser Part. Beams* **22**, 307–314.

Baton, S.D., Baldis, H.A. Jalinaud, T. & Labaune, C. (1993). Fine-scale spatial, and temporal structure of second-harmonic emission from an underdense plasma. *Europhys. Lett*. **23**, 191–196.

Brandi, F., Giammanco, F. & Ubachs, W. (2006). Spectral redshift in harmonic generation from plasma dynamics in the laser focus. *Phys. Rev. Lett*. **96**, 123904.

Brandi, H.S., Manus, C. & Mainfray, G. (1993). Relativistic self-focusing of ultra intense laser pulses in inhomogeneous underdense plasmas. *Phys. Rev. E* **47**, 3780–3783.

Canaud, B., Fortin, X., Garaude, F., Meyer, C. & Philippe, F. (2004). Progress in direct-drive fusion studies for the Laser Mégajoule. *Laser Part. Beams* **22**, 109–114.

Chen, Z.L., Unick, C., Vafaei-Najafabadi, N., Tsui, Y.Y., Fedosejevs, R., Naseri, N., Masson-Laborde, P.E. & Rozmus, W. (2008). Quasi-monoenergetic electron beams generated from 7 TW laser pulses in N-2 and He gas targets. *Laser Particle Beams* **26**, 147–155.

Davis, J., Petrov, G.M. & Velikovich, A.L. (2005). Dynamics of intense laser channel formation in an underdense plasma. *Phys. plasma* **12**, 123–102.

Deutsch, C., Furukawa, H., Mima, K., Murakami, K.M. & Nishihara, K. (1996). Interaction physics of the fast ignitor concept. *Phys. Rev. Lett*. **77**, 2483.

Esarey, E., Ting, A., Sprangle, P., Umstadter, D. & Liu, X. (1993). Nonlinear analysis of relativistic harmonic generation by intense lasers in plasmas. *IEEE Trans. Plasma Sci*. **21**, 95–104.

Ganeev, R.A., Suzuki, M., Baba, M. & Kuroda, H. (2007). High-order harmonic generation from laser plasma produced by pulses of different duration. *Phys. Rev. A* **76**, 023805.

Gibbon, P. (1997). High-order harmonic generation in plasmas. *IEEE J. Quantum Electron*. **33**, 1915.

Giulietti, D., Galimberti, M., Giulietti, A., Gizzi, L.A., Labate, L. & Tomassini, P. (2005). The laser-matter interaction meets the high energy physics: Laser-plasma accelerators and bright X-ray sources. *Laser Part. Beams* **23**, 309–314.

Gupta, M.K., Sharma, R.P. & Mahmoud, S.T. (2007). Generation of plasma wave and third harmonic generation at ultra relativistic laser power. *Laser part. Beams* **25**, 211–218.

Hafeez, S., Shaikh, N.M. & Baig, M.A. (2008). Spectroscopic studies of Ca plasma generated by the fundamental, second, and third harmonics of a Nd:YAG laser. *Laser Part. Beams* **26**, 41–50.

Hora, H. (2007). New aspects for fusion energy using inertial confinement. *Laser Part. Beams* **25**, 37–45.

Huillier, A.L. & Balcou, P. (1993). Higher order harmonic generation in rare gases with a 1-ps 1053–nm laser. *Phys. Rev. Lett*. **70**, 1935.

Imasaki, K. & Li, D. (2008). An approach of laser induced nuclear fusion. *Laser Particle Beams* **26**, 3–7.

Karmakar, A. & Pukhov, A. (2007). Collimated attosecond GeV electron bunches from ionization of high-Z material by radially polarized ultra-relativistic laser pulses. *Laser Part. Beams* **25**, 371–377.

Kruer, W.L. (1988). *The Physics of Laser Plasma Interaction*, New York: Addison – Wesley Publishing Company.

Kuehl, T., Ursescu, D., Bagnoud, V., Javorkova, D., Rosmej, O., Cassou, K., Kazamias, S., Klisnick, A., Ros, D., Nickles, P., Zielbauer, B., Dunn, J., Neumayer, P., Pert, G. & Team, P.

(2007). Optimization of the non-normal incidence, transient pumped plasma X-ray laser for laser spectroscopy and plasma diagnostics at the facility for antiproton and ion research (FAIR). *Laser Particle Beams* **25**, 93–97.

Lemoff, B.E., Yin, G.Y., Gordan, C.L., Barty, C.P.J. & Harris, S.E. (1995). Demonstration of 10-Hz femptosecond-pulse-driven XUV laser at 41.8 nm in Xe IX. *Phys. Rev. Lett*. **74**, 1574.

Liu, M., Guo, H., Zhou, B., Tang, L., Liu, X. & Yi, Y. (2006). Comparison of ponderomotive self-channeling and higher order relativistic effects on intense laser beams propagating in plasma channels. *Phys. Lett. A* **352**, 457–461.

Liu, X., Umstadter, D., Esarey, E. & Ting, A. (1993). Harmonic generation by an intense laser pulse in neutral and ionized gases. *IEEE Trans. Plasma Sci*. **21**, 90.

Malka, V., Modena, A., Najmudin, Z., Dangor, A.E., Clayton, C.E., Marsh, K.A., Joshi, C., Danson, C., Neely, D. & Walsh, N. (1997). Second harmonic generation and its interaction with relativistic plasma wave driven by forward Raman instability in underdense plasmas. *Phys. Plasmas* **4**, 1127–1131.

Merdji, H., Guizard, S., Martin, P., Petite, G., Quéré, F., Carré, B., Hergott, J.F., Déroff, L., Salières, P., Gobert, O., Meynadier, P. & Perdrix, M. (2000). Ultrafast electron relaxation measurements on a-SiO2 using high-order harmonics generation. *Laser Part. Beams* **18**, 489–494.

Meyer, J. & Zhu, Y. (1987). Second harmonic emission from an underdense laser produced plasma and filamentation. *Phys. Fluids* **30**, 890.

Mori, W.B., Decker, C.D. & Leemans, W.P. (1993). Relativistic harmonic content of nonlinear electromagnetic waves in underdense plasmas. *IEEE Trans. Plasma Sci*. **21**, 110.

Neff, S., Knobloch, R., Hoffmann, D.H.H., Tauschwitz, A. & Yu, S.S. (2006). Transport of heavy-ion beams in a 1 m free-standing plasma channel. *Laser Part. Beams* **24**, 71–80.

Neumayer, P., Bock, R., Borneis, S., Brambrink, E., Brand, H., Caird, J., Campbell, E.M., Gaul, E., Goette, S., Haefner, C., Hahn, T., Heuck, H.M., Hoffmann, D.H.H., Javorkova, D., Kluge, H.J., Kuehl, T., Kunzer, S., Merz, T., Onkels, E., Perry, M.D., Reemts, D., Roth, M., Samek, S., Schaumann, G., Schrader, F., Seelig, W., Tauschwitz, A., Thiel, R., Ursescu, D., Wiewior, P., Wittrock, U. & Zielbauer, B. (2005). Status of PHELIX laser and first experiments. *Laser Part. Beams* **23**, 385–389.

Nuzzo, S., Zarcone, M., Ferrante, G. & Basile, S. (2000). A simple model of high harmonic generation in a plasma. *Laser Part. Beams* **18**, 483–487.

Ozaki, T., Bom, L.B.E., Ganeev, R., Kieffer, J.C., Suzuki, M. & Kuroda, H. (2007). Intense harmonic generation from silver ablation. *Laser Part. Beams*, **25**, 321–325.

Ozaki, T., Bom, L.E. & Ganeev, R.A. (2008). Extending the capabilities of ablation harmonics to shorter wavelengths and higher intensity. *Laser Part. Beams* **26**, 235–240.

Ozaki, T., Kieffer, J.C., Toth, R., Fourmaux, S. & Bandulet, H. (2006). Experimental prospects at the Canadian advanced laser light source facility. *Laser Part. Beams* **24**, 101–106.

Regan, S.P., Bradley, D.K., Chirokikh, A.V., Craxton, R.S., Meyerhofer, D.D., Seka, W., Short, R.W., Simon, A., Town, R.P., Yaakobi, B., Carill III J.J. & Drake, R.P. (1999). Laser-plasma interactions in long-scale-length plasmas under direct-drive National Ignition Facility conditions. *Phys. Plasmas* **6**, 2072.

Schifano, E., Baton, S.D., Biancalana, V., Giuletti, A., Giuletti, D., Labaune, C. & Renard, N. (1994). Second harmonic emission from laser-preformed plasmas as a diagnostic for filamentation in various interaction condition. *Laser Part. Beams* **12**, 435–144.

Shi, Y.J. (2007). Laser electron accelerator in plasma with adiabatically attenuating density. *Laser Part. Beams* **25**, 259–265.

Solem, J.C., Luk, T.S., Boyer, K. & Rhodes, C.K. (1989). Prospects for X-ray amplification with charge-displacement self-channeling. *IEEE J. Quantum Electron*. **25**, 2423.

Stamper, J.A., Lehmberg, R.H., Schmitt, A., Herbst, M.J., Young, F.C., Gardener, J.H. & Obenschain, S.P. (1985). Evidence in the second harmonic emission for self-focusing of a laser pulse in a plasma. *Phys. Fluids* **28**, 2563.

Tajima, T. & Dawson, J.M. (1979). Laser electron accelerator. *Phys. Rev. Lett*. **43**, 267.

Yu, W., Yu, M.Y., Xu, H., Tian, Y.W., Chen, J. & Wong, A.Y. (2007). Intense local plasma heating by stopping of ultrashort ultraintense laser pulse in dense plasma. *Laser Part. Beams* **25**, 631–638.

Zeng, G., Shen, B., Yu, W. & Xu, Z. (1996). Relativistic harmonic generation excited in the ultrashort laser pulse regime. *Phys. Plasmas* **3**, 4220.